1956-05

Nuclear energy levels in Mn-56

Green, John W.; Smith, Albert James

NUCLEAR ENERGY LEVELS IN Mn^{56}

John W. Green

and

Albert J. Smith

NUCLEAR ENERGY LEVELS IN Mn^{56}

by

John W. Green

B.S., United States Naval Academy
(1949)

and

Albert J. Smith
B.S., University of South Carolina
(1946)

S.B., Massachusetts Institute of Technology
(1947)

SUBMITTED IN PARTIAL FULFILLMENT OF

THE REQUIREMENTS FOR THE DEGREE OF

MASTER OF SCIENCE

at the

MASSACHUSETTS INSTITUTE OF TECHNOLOGY

(1956)

Signature of Authors_____

Department of Physics, May 21, 1956

Certified by_____
Thesis Supervisor

Accepted by_____
Chairman, Departmental Committee on Graduate Students

NUCLEAR ENERGY LEVELS IN Mn^{56}

by

John W. Green and Albert J. Smith

Submitted to the Department of Physics on May 21, 1956 in partial fulfillment of the requirements for the degree of Master of Science.

ABSTRACT

The MIT-ONR electrostatic generator and broad-range spectrograph were employed to investigate the nuclear energy levels of Mn^{56} by means of the $Mn^{55}(d,p)Mn^{56}$ reaction. Mn^{55} targets were bombarded with 7.006-Mev deuterons, and the proton spectra were observed at laboratory angles of 10, 30, and 60 degrees. Proton groups corresponding to the ground state (Q_o = 5.047 $\pm$ 0.007 Mev) and 107 excited levels were observed. Of particular interest are previously unreported low-lying excited levels at 0.025 Mev, 0.335 Mev, and 0.449 Mev. A discussion of the many problems and techniques involved in the preparation of thin targets is appended.

Supervisor: W. W. Buechner

Title: Associate Professor of Physics

ACKNOWLEDGMENTS

The authors are indebted to the entire staff of the High Voltage Laboratory for its friendly interest in the accomplishment of this work.

We particularly wish to thank Professor W. W. Buechner for suggesting the field of investigation and patiently supervising our efforts. Mr. A. Sperduto devoted much time to briefing us on the operation of equipment. We are also very grateful to him and to Dr. C. P. Browne, Dr. H. A. Enge, and Mr. R. D. Sharp for their thoughtful consideration of our many problems.

The valuable assistance given us by Miss Sylvia Darrow, Miss Estelle Freedman, and Mr. Wilton Tripp in the tedious and demanding job of plate counting and the cooperation of Mrs. Grace Rowe in the preparation of the plots are both much appreciated.

Finally, we wish to thank Mrs. Mary E. White for her patience and understanding in so capably preparing the manuscript.

TABLE OF CONTENTS

TABLE OF FIGURES

I. INTRODUCTION

The purpose of this work was to investigate the energy levels of Mn^{56} by means of the nuclear reaction $Mn^{55}(d,p)Mn^{56}$.

Experimental determination of the exact location of the energy levels found in atomic nuclei provides one of the fundamentals upon which is gradually being developed the physical model of the nucleus and perhaps eventually an understanding of nuclear forces.

Much effort has been devoted to studying the energy levels of light nuclei, since, in the past, the available bombarding energies were equal to or less than the barrier heights of the light nuclei. Gradually machines of higher energies have become available, so that the medium-mass nuclei can be attacked. The MIT-ONR generator produces such higher energies. Coupled with this increase in bombarding energy, the High Voltage Laboratory can also utilize its broad-range spectrograph which makes possible the discovery of many heretofore unresolved levels.

The nucleus Mn^{56} was chosen for this investigation, because it lies in the newly opened up region of the medium-mass nuclei; and, although it has been investigated previously by means of (n,γ) and (d,p) reactions, its entire spectrum of levels up to an excitation of 7 Mev could be studied at high resolution. In addition, since the level structure of Fe^{56} and several other nuclides in the same region of the periodic table have recently been studied with similar excitations and identical resolution, a comparison

with Mn^{56} would surely be of interest. Furthermore, theory predicts a high density of energy levels for Mn^{56}, because it is an odd-odd nucleus; and, since this prediction had not been verified by previous experiments, it proved an additional inducement. Manganese is particularly advantageous as a target element because it is monoisotopic, making the assignment of levels unique.

In 1947, using 3.68-Mev deuterons from a cyclotron, A. B. Martin[1] observed the proton spectrum of $Mn^{55}(d,p)Mn^{56}$ by means of range measurements. He determined the energies for six proton groups and reported the Q-values and energies for the ground state and five excited levels. In 1950, A. Y. Abramov[2] bombarded Mn^{55} with 3.8-Mev deuterons and observed proton groups corresponding to the ground state and five excited levels. In the same year, W. D. Whitehead and N. D. Heydenburg[3] carried out an investigation of the same reaction with 3.0-Mev deuterons and reported the ground state and six excited levels. In 1952, B. Hamermesh and V. Hummel[4] reported four capture gamma rays from the $Mn^{55}(n,\gamma)Mn^{56}$ reaction, as observed by a one-crystal scintillation counter. Pair-spectrometer measurements reported in 1953 by G. A. Bartholomew and B. B. Kinsey[5] yielded eighteen capture gamma rays, which were arranged in a tentative decay scheme. In 1954, M. Reier and M. M. Shamos[6], using a one-crystal scintillation counter, observed four capture gammas from the $Mn^{55}(n,\gamma)Mn^{56}$ reaction. All except the last are discussed by Bartholomew and Kinsey[5], and all data up to 1955 are summarized in Nuclear Level Schemes (TID-5300) June 1955.[7]

II. APPARATUS AND EXPERIMENTAL PROCEDURE

APPARATUS

In this experiment, the MIT-ONR electrostatic generator was employed as the source of a collimated beam of accelerated deuterons. This generator is a large, vertical, pressure-insulated Van de Graaff accelerator that operates in the voltage range of 4.0 to 8.5 Mev. A schematic of the generator and some of the associated equipment is presented in Figure 1.

After emerging from the accelerating tube, the deuteron beam is deflected 90 degrees by the beam analyzing magnet and proceeds in a horizontal direction. The beam analyzing magnet is actually a momentum filter, but it acts effectively as an energy filter, since the mass of the deuteron is accurately known. Adjustable shims at the entrance and exit slit faces of the magnet are positioned so as to focus the beam on a set of defining slits located 185 cm from the exit fact of the analyzer. The slit jaws are insulated, and the current collected on them is used to control a conventional voltage stabilizing device utilizing corona directed at the generator terminal[8].

Upon leaving the slit system, the deuteron beam impinges on the target located in the target chamber. In this experiment, several different nuclear reactions take place; for example, $Mn^{55}(d,p)Mn^{56}$ and $Mn^{55}(d,d)Mn^{55}$. Product particles of these reactions are emitted in all directions. An exit can be so positioned that only particles

emitted at the desired laboratory angle can leave the target chamber. Such particles then pass through the entrance slit to the magnet of the broad-range spectrograph, which is capable of rotating through laboratory angles from zero degrees to 130 degrees. The magnetic field acting upon the emitted particles produces a momentum spectrum which is well resolved within an energy range of 2.4. Three NTA Eastman nuclear track plates (10 inches x 2 inches), placed end to end along the curved focal surface of the broad-range spectrograph, record this momentum spectrum. The photographic plates are accurately indexed before and after exposure. The plateholder can be translated within the camera box so that several exposures can be made on each set of plates. Figure 2 is a schematic of the target chamber, the broad-range spectrograph, and the camera box; while Figure 3 illustrates the ion optics of the broad-range spectrograph and the photographic plates. Figure 4 is a photograph of the above-described equipment.

Stabilized, three-phase, rectifier circuits, designed by H. A. Enge, provide power for both the 90-degree beam analyzing magnet and the broad-range spectrograph. The fields produced by each of these magnets can be maintained constant to 1 part in 100,000. These magnetic fields are measured by means of nuclear magnetic fluxmeters[9].

After passing through the target, the deuteron beam is collected by a Faraday cage. A current integrator[10] then activates a

Fig. 1. Positive Ion Accelerator at MIT

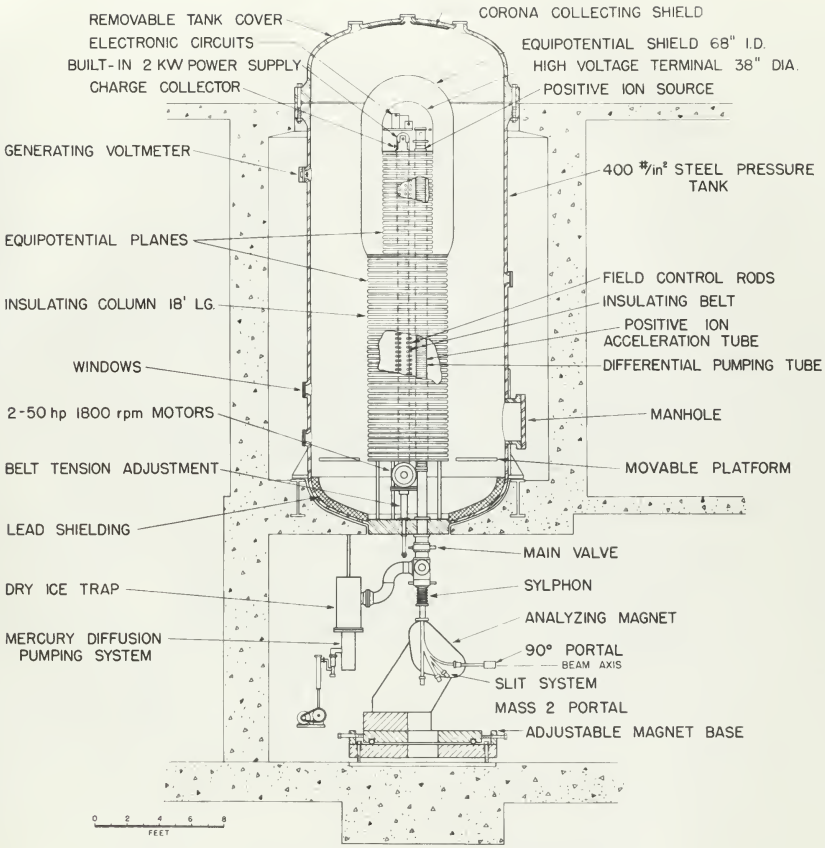

POSITIVE ION ACCELERATOR FOR M.I.T.

Fig. 2. Schematic of Target Chamber Spectrograph and Camera Box.

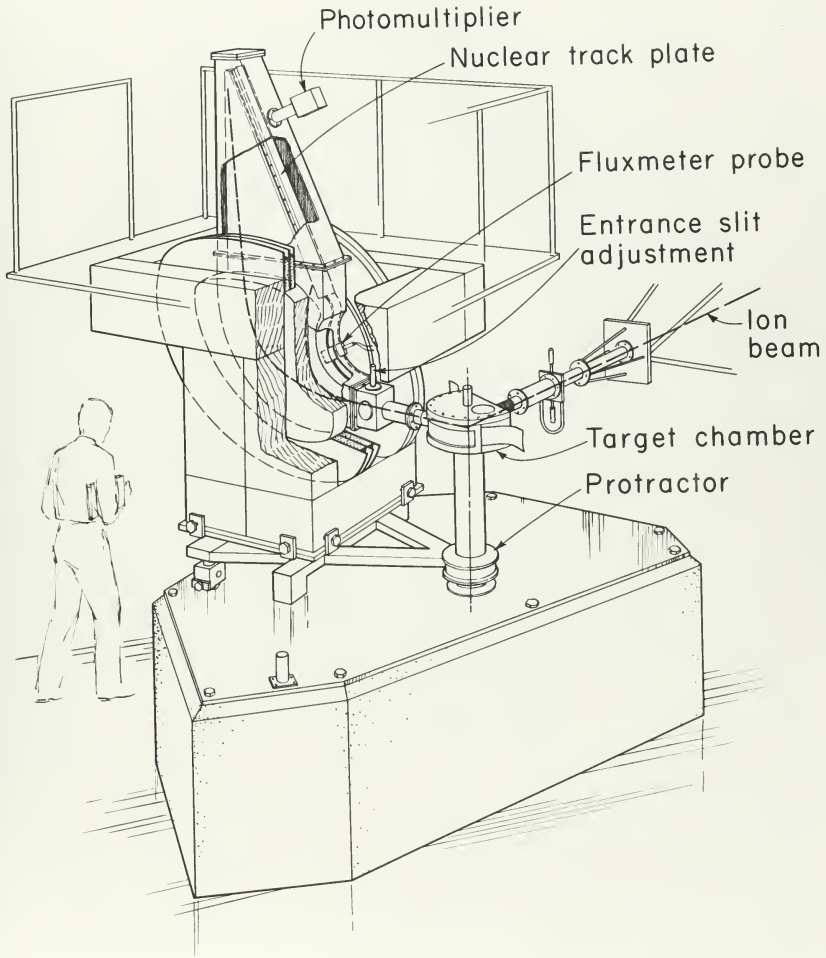
Photomultiplier
Nuclear track plate
Fluxmeter probe
Entrance slit adjustment
Ion beam
Target chamber
Protractor

Fig. 3. Geometrical Features
of the Spectrograph.

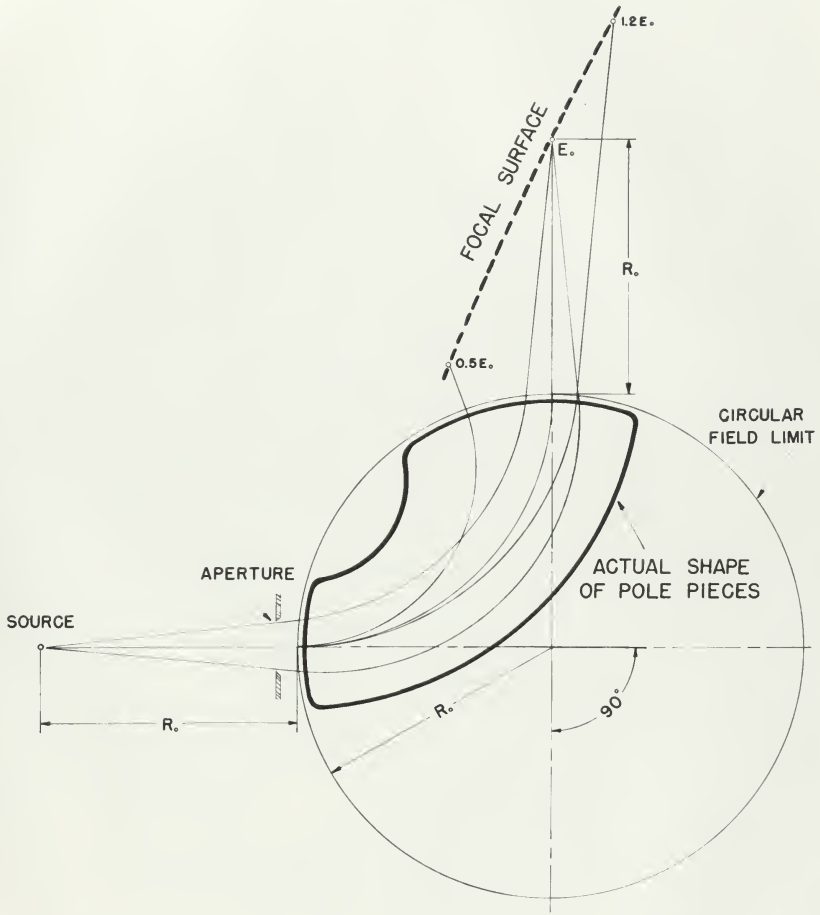
1.2E₀
FOCAL SURFACE
E₀
R₀
0.5E₀
CIRCULAR
FIELD LIMIT
ACTUAL SHAPE
OF POLE PIECES
APERTURE
SOURCE
R₀
R₀
90°

Fig. 4. Photograph of Equipment
in Target Room.

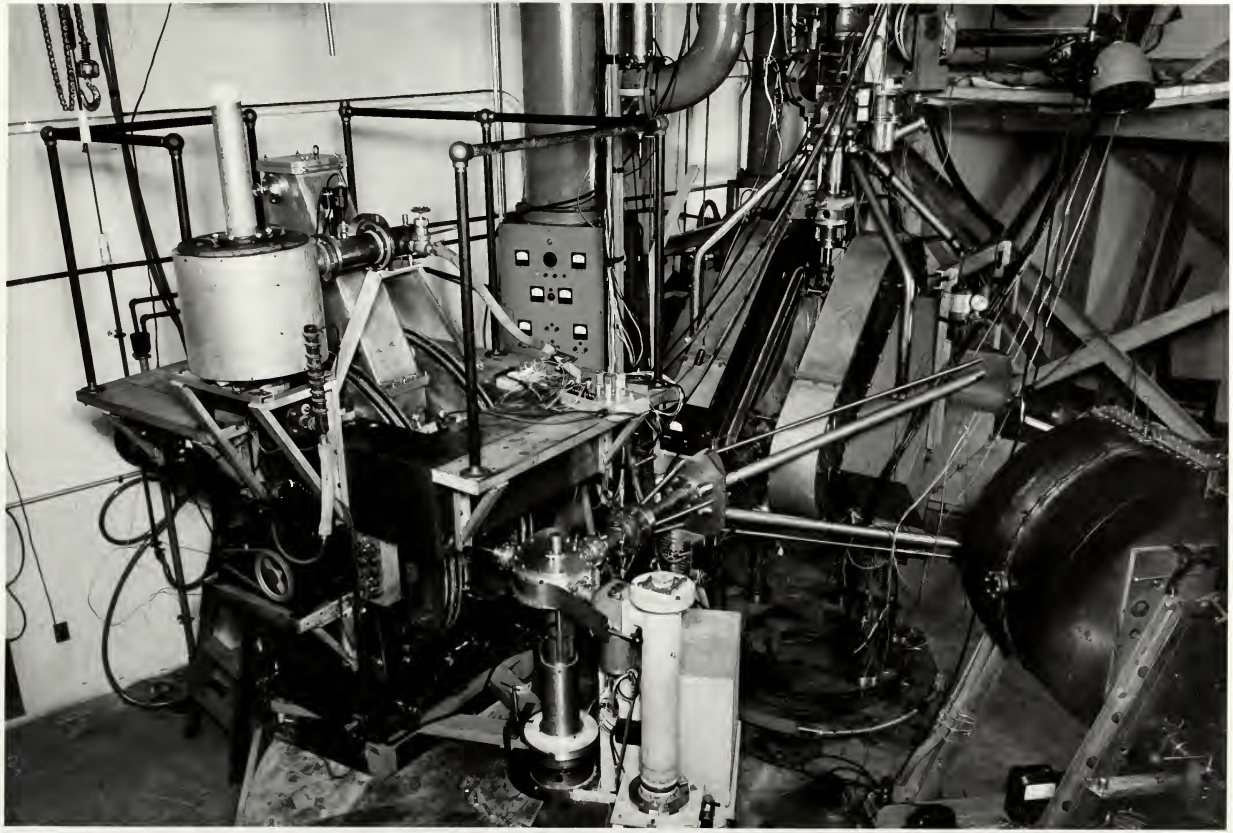

mechanical register and a sensitive microammeter. The register displays total exposure in microcoulombs while the microammeter measures the beam current.

Since the broad-range spectrograph inherently provides an energy resolution ($E/\Delta E$) of the proton groups of the order of 800 to 1600[9], this advantage should not be forfeited by employing thick targets. The exacting art of thin-target making is consequently given considerable emphasis at the High Voltage Laboratory. The targets for this investigation consisted of spectroscopically pure Mn^{55} (99.99 percent pure) evaporated on a thin backing of Formvar. For details on the many problems involved in target making, see Appendix I.

The nuclear track plates are developed by normal photographic techniques. The tracks are then counted by means of binocular microscopes, using 12-power eyepieces in conjunction with either 20-power or 43-power objectives. These microscopes have been provided with specially constructed movable stages that make it possible to measure distances along the plate to $\pm$ 0.01 mm, as well as to scan up and down a $\frac{1}{2}$ mm strip of the plate. Grid-type reticules in the eyepiece define a $\frac{1}{2}$ mm x $\frac{1}{2}$ mm area with 20-power objective and a $\frac{1}{4}$ mm x $\frac{1}{4}$ mm area with 43-power objective.

EXPERIMENTAL PROCEDURE

Nine experimental runs were conducted, in which the following experimental conditions were varied as indicated:

1. Type of Reaction. The nuclear reaction to be investigated could be controlled through the presence or absence of aluminum foil over the portion of the plates exposed; that is, since foil of the proper thickness is opaque to both deuterons and alpha particles, it was used when it was desired to record the (d,p) reaction only. A greater thickness of foil is required on the plates receiving the higher energy portions of the proton spectrum.

2. Laboratory angle. The laboratory angle was varied by rotating the spectrograph around the target chamber.

3. Input energy. The input deuteron energy was controlled by adjusting the field strength of the beam analyzing magnet.

4. The observed spectrum. The field strength of the broad-range spectrograph was adjusted so that at each laboratory angle the ground-state proton group would appear near the high-energy end of the plates. In the runs used to determine input deuteron energy, at $\theta = 60$ and $\theta = 30$ degrees, the spectrograph was adjusted so that the (d,d) elastic group would appear near the high-energy end of the plates.

5. Exposure. The total exposure was observed on the current integrator register and was varied to give the desired yield and to insure that each peak would be countable on some run.

Tabulated data on the experimental conditions present in the nine runs follow:

TABLE I

Experimental Conditions

Run No.	Analyzer Field (Gauss)	Spectrograph Field (Gauss)	Reaction	Lab Angle	Exposure μc	Foil
1	8945	8955	(d,p)	10	1000	Yes
2	8945	8955	(d,p) (d,d)	10	10	No
3	8945	8955	(d,p) (d,d)	10	1	No
4	8945	8933	(d,p)	60	1000	Yes
5	8945	9489	(d,d)	60	25	No
6	8945	9489	(d,d)	60	5	No
7	8945	8870	(d,p)	30	1000	Yes
8	8945	9610	(d,d)	30	3	No
9	8945	8870	(d,p)	30	100	Yes

The nuclear particle tracks left by protons, deuterons, and alpha particles can usually be distinguished by their ionization density and length. The photographic plates were firmly held to the microscope stage after the index mark had been accurately aligned with the distance gauge. The stage was then positioned to bring $\frac{1}{2}$ mm strips of the plates successively under the objective at intervals of $\frac{1}{2}$ mm ($\frac{1}{4}$ mm when passing through peaks). The total number of counts in each strip was recorded on a counter and tabulated on the data sheet versus plate distance. When peaks were too dense to be countable with the 20-power objective, the 43-power objective was substituted. If the peaks were still uncountable, the peak was counted on a zone which had received a shorter exposure.

The complete proton spectra were plotted separately for both the 10- and 30-degree runs in order to give an overall picture of the proton groups present. Contaminant groups appeared at different distances on both plots, and since they masked portions of the manganese level structure on each of the 10- and 30-degree plots, corresponding portions of the 60-degree data were plotted to resolve any uncertainties as to identification. Comparison of the overall plots provided a means of estimating which peaks represented identical manganese levels. Such peaks were replotted to a greatly expanded distance scale and the distance corresponding to the point along the high-energy edge of the peak at which the proton count was one-third of the maximum was recorded.

The one-third height distance is considered to define most accurately the group location for three reasons:

1. Experience has shown that this point falls in the most linear portion of the peak.

2. This point appears to be least dependent on target thickness.

3. This point was used in calibrating the spectrograph against the Po-α spectrum because of (1) and (2).

III. DATA ANALYSIS

COMPUTATIONS

The foundation upon which the mathematics of this investigation is based is the familiar Q-equation.[11]

$$Q = \left(\frac{M_T + M_O}{M_T}\right)E_O - \left(\frac{M_T - M_i}{M_T}\right)E_i + \left(\frac{E_i^2 + E_O^2 - E_T^2}{2M_T c^2}\right)$$

$$- \frac{2(M_i E_i M_O E_O)^{\frac{1}{2}}}{M_T} \cos\theta \left(1 + \frac{E_i}{2M_O c^2}\right)^{\frac{1}{2}} \left(1 + \frac{E_O}{2M_O c^2}\right)^{\frac{1}{2}} \quad (1)$$

where

Q = nuclear disintegration energy = total change in rest mass of the reaction

M_i = mass of incident particle

M_O = mass of observed particle

M_T = mass of residual nucleus

E_O = energy of the observed particle

E_i = energy of the incident particle

θ = laboratory angle at which observed particle is emitted.

$E_T = E_i - E_O + Q$ = energy of residual nucleus.

Since $E_i \ll 2 M_i c^2$ and $E_O \ll 2M_O c^2$, Eq. (1) can be rewritten after expanding the last two factors in parentheses by the binomial expansion and neglecting second-order and higher terms:

$$Q = \left(\frac{M_r + M_o}{M_r}\right)E_o - \left(\frac{M_r - M_i}{M_r}\right)E_i - \frac{2\cos\theta\sqrt{M_iE_iM_oE_o}}{M_r} + \delta_{rel}, \quad (2)$$

where

$$\delta_{rel} \approx \frac{1}{2M_rc^2}\left[E_i^2 + E_o^2 - E_r^2 - \cos\theta\sqrt{M_iM_oE_iE_o}\left(\frac{E_i}{M_i} + \frac{E_o}{M_o}\right)\right]$$

and M_rc^2 is expressed in the same energy units as E_o and E_i.

δ_{rel} did not exceed 0.2 kev in any of the reactions studied, and, since this value is well within the experimental errors, it was neglected.

Since the Q-value of a reaction depends only upon the difference in total rest masses before and after reactions, it is possible to identify the proton groups by varying either the input energy or the laboratory angle, and noting those groups for which the Q-value remains constant when Eq. (2) is solved for the $Mn^{55}(d,p)Mn^{56}$ reaction.

The masses M_i, M_o, M_r were taken from tables compiled mainly from the published values of K. T. Bainbridge[12].

E_i was computed by solving Eq. (2) in either of the following cases where the Q-value was already well known:

1. $Mn^{55}(d,d)Mn^{55}$ Q = 0
2. $C^{12}(d,p)C^{13}$ Q = 2.722 Mev.

Data were available for either reaction 1 or 2 for each of the experimental runs.

To find E_o, the distance, d, of the proton group along the plate was determined from the expanded plots of the peaks as described in Part II. The radius of curvature of this group was next found by entering a set of ρ versus d tables[13] with d and interpolating for ρ. The spectrograph induction, B, was determined from the known frequency of the resonance fluxmeter, f, by means of the following conversion:

$$B(\text{kilogauss}) = \frac{f(\text{kilocycles})}{1.6546 \frac{(\text{kilocycles})}{(\text{kilogauss})}} .$$

The resulting magnetic rigidity ($B\rho$) was used as the argument to enter a set of "charged-particle energies versus $B\rho$" tables compiled by H. A. Enge[14]. The values in this table had been computed using the relativistically correct relationship:

$$E_o = m_o c^2 \left(\sqrt{1 + \left(\frac{ZeB\rho}{m_o c}\right)^2} - 1 \right)$$

where,

m_o = rest mass of the particle

e = electrostatic unit of charge

Z = charge of the particle

c = velocity of light.

Knowing M_1, M_0, M_r, cos θ, E_1, and E_0, it is possible to determine the Q-value by solving Eq. (2). Since over 300 proton peaks had to be expanded in the course of this work, it was decided that carrying out this solution repeatedly would be too time-consuming. The Q-equation had already been coded by H. A. Enge[15] for solution by the IBM 650 operated by the Statistical Services Section of the Laboratory for Nuclear Science. Consequently, it was only necessary to provide the IBM with constants appropriate to the specific reaction, laboratory angle, and input deuteron energy. The IBM 650 then computed values of Q and proton energy for integral values of d in centimeters. Q versus d so nearly approximates a straight line over wide ranges that the extremely small amount of inaccuracy introduced through linear interpolation is well within experimental error.

The target employed for the 30-degree run proved to be the thinnest and gave the best resolved peaks. The targets employed for the 10- and 60-degree runs yielded broader peaks typical of thicker targets. It was therefore decided to normalize the 10- and 60-degree runs to the 30-degree run and use them for identification purposes only. This normalization was accomplished by comparing the Q-values of four well-separated, high-intensity proton groups computed at each angle. The Q-values computed for the 10-degree and 60-degree runs were a constant, 4 kev and 9 kev, respectively, below the corresponding Q-values calculated for the

proton groups of the 30-degree run. Hence, 4 kev and 9 kev were added to all Q-values calculated for the 10-degree run and the 60-degree run, respectively, before comparing with the 30-degree run for identification.

Identification of Mn^{56} levels was considered as positive when the Q-values agreed within 10 kev for proton groups suspected to be identical on two runs, provided that the peaks in question were adequately resolved from other peaks. In Appendix II, an analysis under the above restrictions, shows that, in order to avoid confusing contaminant levels with those of Mn^{56}, the target should be free of any appreciable amount of contaminants of atomic mass 47 to atomic mass 68.

A spectroscopic analysis (see Appendix I) of the manganese used in the 30- and 60-degree runs indicates that very faint lines attributed to Mg, Cu, and Ca were found. Magnesium and calcium do not have masses in the range A = 47 to 68, and, while copper does lie in this range, it is believed that an amount of copper corresponding to very faint lines would not produce sufficient reaction yield to be detectable in the proton spectrum.

Corresponding energy levels, E_n, could be determined for each Q-value, Q_n, from the relationship:

$$E_n = Q_o - Q_n ,$$

where

Q_o = the ground-state Q-value.

The excitation energies, E_n, are preferred in comparing the present work with the findings of previous investigations, since in such a comparison the systematic errors in the Q-values tend to cancel out.

PROBABLE ERRORS

Sources of Experimental Errors:

1. Uncertainty in deuteron energy.

2. Uncertainty in proton energy because of losses in target.

3. Finite width of beam.

4. Aberration in broad-range spectrograph.

5. Variation of the field induction at position of fluxmeter, as compared with average field induction in proton path.

6. Plate counting (setting of index marks, missed counts, backlash).

7. Indexing of plates, deviation of these plates from the focal plane, and slipping in the plateholder.

8. Errors in experimentally determined value of $B\rho$ for polonium alpha particles used for calibrating the broad-range spectrograph.

E. N. Strait and H. A. Enge[16] have made an exhaustive study of experimental errors that occur in this Laboratory. Using this as a guide in conjunction with the Laboratory's experience, it was

possible to assign an error of $\pm$ 7 kev to each Q-value. Since the input and output energies were both measured by the broad-range spectrograph, the systematic errors are partly canceled in the Q-equation.

If the total error in the Q-values is considered to be purely random, the total probable error in the excitation energy is taken as the square root of the sum of squares of the two Q-value total errors. This would lead to a probable error of 10 kev in each excitation energy. However, any systematic errors in the Q-values would tend to reduce the probable error in the energy levels. It is therefore considered reasonable to assign 10 kev as the limit of error in the energy levels.

IV. RESULTS

FINDINGS

Proton groups corresponding to the ground state and 107 excited levels of the nucleus Mn^{56} were determined by the means discussed in parts II and III. Figures 5a, b, c, and d present the proton spectrum observed in the experimental run conducted at a laboratory angle of 30 degrees. Quite a few of the proton groups observed display a tendency to separate into further levels, as can be seen especially in Figures 5c and d. No attempt was made, however, to determine levels in the cases where resolution was inadequate. Level No. 93, marked with an asterisk, was observed only on the 30-degree run, being obscured by a contaminant peak in both the 10- and 60-degree runs. It is included in the levels reported, because it is so intense and so well resolved and gives every appearance of being a bona fide level.

Table II is a tabulation of present findings. Bartholomew and Kinsey's findings[5] are included for comparison. An asterisk indicates levels derived from their gamma rays but not definitely predicted on their tentative decay scheme.

Proton Spectrum $Mn^{55}(d,p)Mn^{56}$ at θ = 30 degrees

(a)

ρ = 49.2 to ρ = 56.3

(b)

ρ = 45.4 to ρ = 49.2

Fig. 5

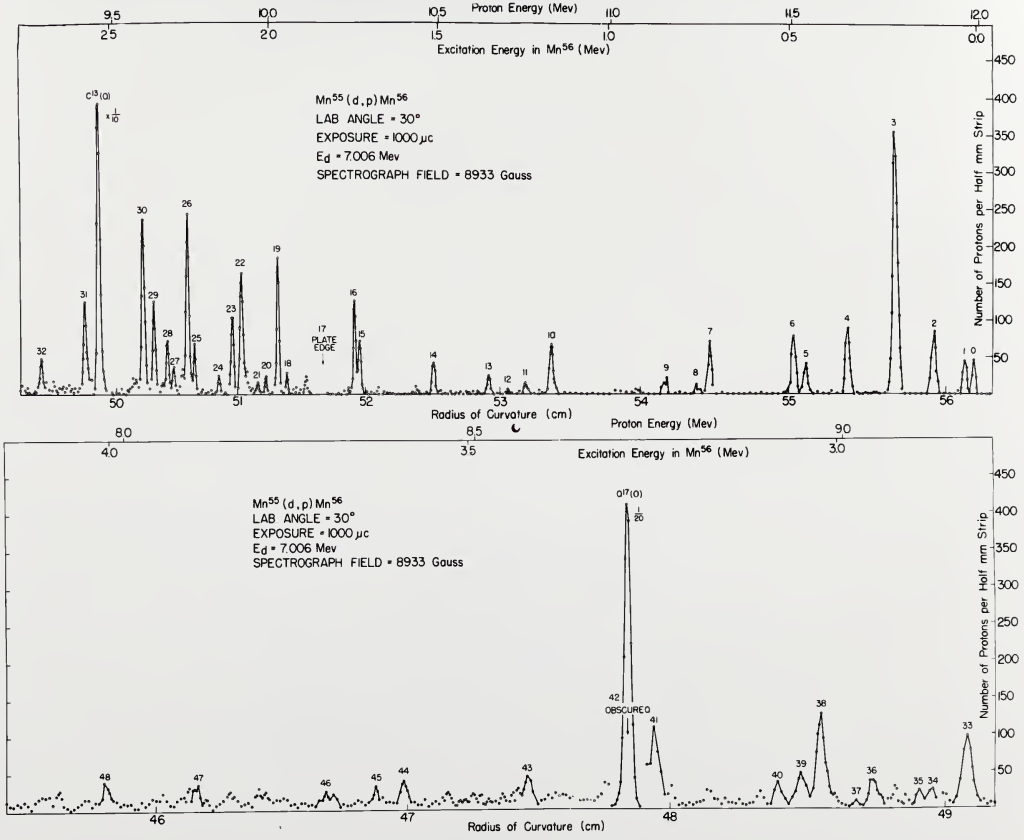
Proton Energy (Mev)
9.5
10.0
10.5
11.0
11.5
12.0
2.5
2.0
1.5
1.0
0.5
0.0
Excitation Energy in Mn56 (Mev)
Mn55 (d,p) Mn56
LAB ANGLE = 30°
EXPOSURE = 1000 μc
Ed = 7.006 Mev
SPECTROGRAPH FIELD = 8933 Gauss
C13 (0)
× 1/10
PLATE EDGE
OBSCURED
Number of Protons per Half mm Strip
Radius of Curvature (cm)
Proton Energy (Mev)
8.0
8.5
9.0
4.0
3.5
3.0
Excitation Energy in Mn56 (Mev)
Mn55 (d,p) Mn56
LAB ANGLE = 30°
EXPOSURE = 1000 μc
Ed = 7.006 Mev
SPECTROGRAPH FIELD = 8933 Gauss
O17 (0)
× 1/20
OBSCURED
Number of Protons per Half mm Strip
Radius of Curvature (cm)

Proton Spectrum $Mn^{55}(d,p)Mn^{56}$ at θ = 30 degrees

(c)

ρ = 41.2 to ρ = 45.6

(d)

ρ = 36.3 to ρ = 41.5

Fig. 5

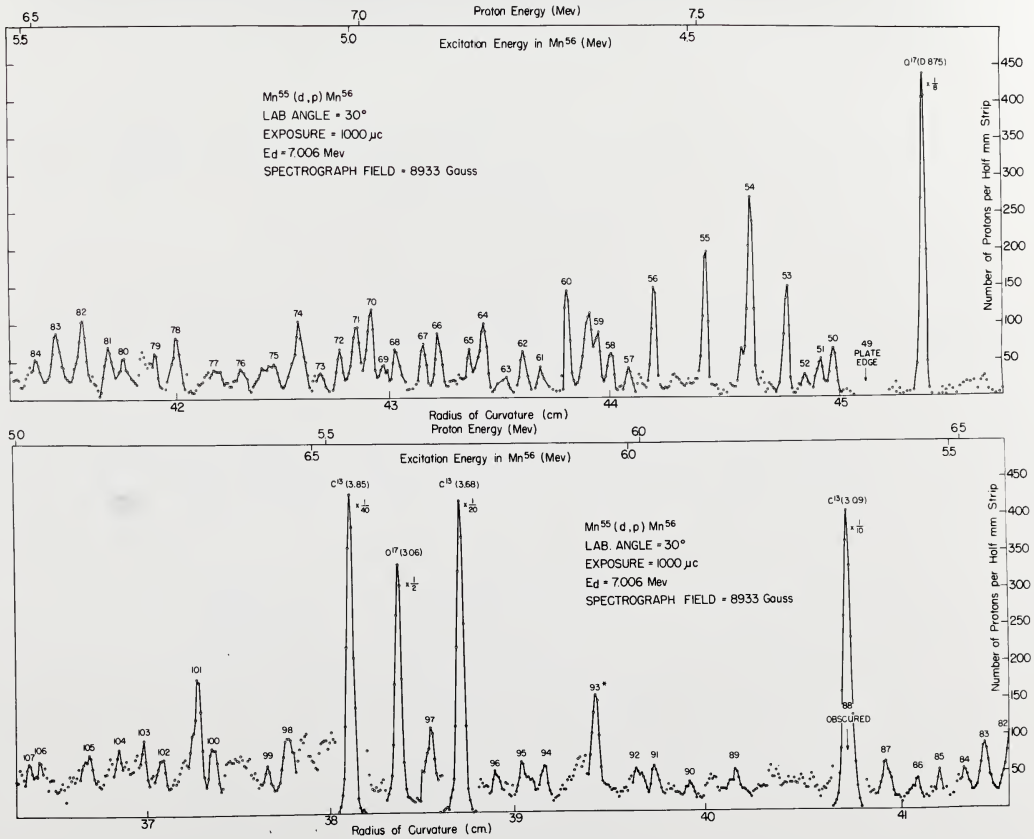
Proton Energy (Mev)
Excitation Energy in Mn56 (Mev)
Mn55 (d,p) Mn56
LAB ANGLE = 30°
EXPOSURE = 1000 μc
Ed = 7.006 Mev
SPECTROGRAPH FIELD = 8933 Gauss
O17(0.875)
PLATE EDGE
Number of Protons per Half mm Strip
Radius of Curvature (cm)
Proton Energy (Mev)
Excitation Energy in Mn56 (Mev)
C13 (3.85)
C13 (3.68)
O17(3.06)
C13(3.09)
OBSCURED
Mn55 (d,p) Mn56
LAB. ANGLE = 30°
EXPOSURE = 1000 μc
Ed = 7.006 Mev
SPECTROGRAPH FIELD = 8933 Gauss
Number of Protons per Half mm Strip
Radius of Curvature (cm)

TABLE II

Level	Rel. Int. (a)	Q(Mev) (b)	E(Mev) (c)	E(Mev) (n,γ) (d)	(e)
0	1.00	5.047	0.000		(A)
1	0.98	5.022	0.025		
2	1.87	4.939	0.108	0.11 ± 0.02	(A,B)
3	7.90	4.840	0.207	0.21 ± 0.01	(A,C)
4	2.00	4.712	0.335		
5	0.91	4.598	0.449		
6	1.74	4.568	0.479	0.48 ± 0.01	(A,D)
7	1.58	4.334	0.713		
8	0.29	4.294	0.753		
9	0.49	4.212	0.835	0.83 ± 0.01*	(A,E)
10	1.49	3.886	1.161	1.15 ± 0.01	(A,F)
11	0.36	3.816	1.231		
12	0.16	3.757	1.290		
13	0.56	3.703	1.344	1.35 ± 0.02*	(A,G)
14	0.93	3.541	1.506	1.49 ± 0.01*	(A,H)
15	1.60	3.321	1.726	1.73 ± 0.01	(A,J)
16	2.80	3.306	1.741		
17	0.65(10^{0})	3.194	1.853		
18	0.64	3.097	1.950		
19	4.09	3.072	1.975		
20	0.53	3.034	2.013		

Level	(a)	(b)	(c)	(d)	(e)
21	0.36	3.009	2.038	2.05 ± 0.01*	(A,K)
22	3.62	2.962	2.085		
23	2.38	2.933	2.114		
24	0.56	2.889	2.158		
25	1.51	2.814	2.233	2.22 ± 0.01	(A,L)
26	5.40	2.794	2.253		
27	0.60	2.749	2.298		
28	1.60	2.729	2.318		
29	2.78	2.688	2.359		
30	5.23	2.660	2.387		
31	2.76	2.470	2.577	2.54 ± 0.02*	(A,N)
32	1.07	2.328	2.719		
33	2.22	2.227	2.820		
34	0.58	2.197	2.850		
35	0.56	2.182	2.865		
36	0.85	2.124	2.923		
37	0.24	2.094	2.953		
38	2.98	2.031	3.016	3.02 ± 0.01*	(A,P)
39	1.07	2.007	3.040		
40	0.82	1.975	3.072		
41	2.36	1.809	3.238		
42	2.22(10°)	1.759	3.288		
43	1.05	1.636	3.411		
44	0.89	1.464	3.583		

Level	(a)	(b)	(c)	(d)	(e)
45	0.73	1.422	3.625		
46	0.58	1.353	3.694		
47	0.78	1.174	3.873		
48	0.87	1.055	3.992		
49	1.99(10°)	0.819	4.228	4.24 ± 0.01*	(P-g)
50	1.47	0.763	4.284		
51	1.16	0.745	4.302		
52	0.69	0.724	4.323		
53	3.33	0.694	4.353		
54	6.00	0.642	4.405		
55	4.38	0.575	4.472		
56	3.33	0.500	4.547	4.55 ± 0.01*	(O-g)
57	0.89	0.466	4.581		
58	1.33	0.438	4.609		
59	2.54	0.418	4.629		
60	3.20	0.372	4.675		
61	0.93	0.340	4.707	4.72 ± 0.02*	(N-g)
62	1.40	0.310	4.737		
63	0.62	0.284	4.763		
64	2.22	0.250	4.797		
65	1.47	0.227	4.820	4.81 ± 0.01*	(M-g)
66	2.00	0.183	4.864		
67	1.62	0.159	4.888		

Level	(a)	(b)	(c)	(d)	(e)
68	1.47	0.123	4.924		
69	1.00	0.105	4.942		
70	2.67	0.081	4.966		
71	2.14	0.061	4.986		
72	1.47	0.035	5.012		
73	0.76	0.010	5.037	5.04 $\pm$ 0.02*	(L-g)
74	2.31	-0.021	5.068		
75	0.96	-0.061	5.108		
76	0.89	-0.109	5.156		
77	0.87	-0.152	5.199	5.21 $\pm$ 0.01*	(K-g)
78	1.82	-0.210	5.257		
79	1.36	-0.247	5.294		
80	1.22	-0.292	5.339		
81	1.56	-0.312	5.359		
82	2.38	-0.355	5.402		
83	1.98	-0.389	5.436		
84	1.20	-0.424	5.471		
85	1.18	-0.468	5.515		
86	0.93	-0.499	5.546		
87	1.45	-0.546	5.593		
88	2.22(10°)	-0.578	5.625		
89	1.00	-0.780	5.827		
90	0.69	-0.851	5.898		

Level	(a)	(b)	(c)	(d)	(e)
91	1.05	-0.906	5.953		
92	0.96	-0.933	5.980		
93*	3.51	-0.999	6.046		
94	1.07	-1.083	6.130		
95	0.98	-1.117	6.164		
96	0.82	-1.159	6.206		
97	2.38	-1.259	6.306		
98	1.62	-1.490	6.537		
99	0.80	-1.521	6.568		
100	1.45	-1.609	6.656		
101	3.78	-1.630	6.677		
102	1.02	-1.687	6.734		
103	1.60	-1.719	6.766		
104	1.33	-1.756	6.803		
105	1.16	-1.803	6.850		
106	0.80	-1.880	6.927		
107	0.98	-1.885	6.932		

(a) Intensity relative to ground state (at 30° except where noted).

(b) Q-value in Mev ± 0.007 (present work).

(c) Excitation in Mev ±0.010 (present work).

(d) Excitation in Mev (Bartholomew and Kinsey).

(e) Gamma rays involved (see Ref. 5; g = ground state).

DISCUSSION OF PRESENT AND PREVIOUS FINDINGS

As can be seen from Table II, the present results include all the excited levels predicted by Bartholomew and Kinsey from computations based on the intense gamma rays that they observed. Agreement is also noted with the levels accompanied by asterisks, which were assigned with less certainty to Bartholomew and Kinsey's tentative decay scheme because they were based on weaker gamma rays.

All but two of the sixteen excited levels indicated in the Mn^{56} nuclear level scheme given in the TID-5300 Summary were found. For both of these cases, as well as for the remainder of the discrepancies between previously reported findings and those of the present work, a reasonable explanation is afforded by the large errors quoted by the previous investigators. For example, Martin[1] reports a 0.110-Mev error and Abramov[2], a 0.100-Mev error with each of their levels.

It is concluded that the theoretical prediction of a high density of nuclear energy levels for the nucleus $_{25}Mn^{56}$ has been verified by this investigation.

SUGGESTIONS FOR FUTURE WORK

The nucleus Mn^{56} offers a promising field for future investigations. Since Mn^{56} is an odd Z, odd N nuclide, an angular distribution study would be of particular interest with a view

toward utilizing stripping theory to assign orbital angular momentum, spin, and parity to excited levels of Mn^{56}. The resultant level scheme can then be used to check predictions based on the shell model.

APPENDIX I

THIN TARGET PREPARATION

GENERAL

Thin targets are of fundamental importance to the work of the High Voltage Laboratory, because it would be extremely inefficient to waste the high-resolution properties of the broad-range spectrograph on an analysis which would already be limited by the relatively large uncertainties introduced by thicker targets.

Target Properties:

1. Thickness. A very thin target is desirable in order that the incident and emerging particles will lose as little energy as possible in traversing it. On the other hand, targets must not be so thin that unreasonably long exposures to the beam are needed to achieve the required yield. This is an excellent example of the constant battle in experimental physics for gaining resolution without sacrificing intensity.

2. Uniformity. The target material may be uniformly spread over the fact of the target, in which case, no matter where it strikes, the incident beam finds the same thickness. On the other hand, the target-making technique employed may result in clumping of the target material in uneven lumps on the face of the target. This has several bad effects: The beam may hit an "opaque" target instead of a "transparent" one; the

beam may strike no material at all; the beam may vary between the last two extremes, in a random fashion, so that no conclusions can be drawn from the length of exposure. In addition, the target is more subject to rupture from uneven heating.

3. Contaminants. While it is practically impossible to avoid contaminants completely, it is usually possible to avoid contaminants that have nearly the same nuclear properties as the target nuclide and would thus be difficult to distinguish from it.

Many contaminants can be avoided by using distilled water in making the Formvar backing discussed later and using "clean" evaporation techniques. The selection of the boat material used in the evaporation process is critical. For a high- or medium-mass target, carbon boats are excellent, since the nuclear levels in carbon are few and well established, For light- and medium-mass nuclide targets, tantalum metal makes an excellent boat, since it does not evaporate too readily and has a large atomic mass (A = 181), making it easier to distinguish from the target material. Furthermore, the high coulomb barrier associated with the high atomic number of tantalum encourages a low reaction yield.

Because the amount of target material is small, it pays to procure the purest material available from a reliable supplier.

As targets become old, they collect surface contaminants in the vacuum system of the machine.

4. Durability. Targets possessing this property should be able to withstand a certain amount of mechanical shock, exposure to the atmosphere, and exposure to reasonable beam currents in the target chamber.

The largest single factor will be the ability of the target to dissipate the heat that occurs in the very localized area where the beam strikes. If the target will not take the beam readily, a special mounting may be devised to enable it to be rotated continuously in the target chamber.

TARGET TYPES

The usual configuration of the target chamber requires that each target be attached to a metal rod about 4 cm long that can be positioned so that the point where the beam strikes the target is accurately known. Since thin targets are fragile, they are usually supported on a backing which may be either solid or transparent.

Solid backings are those which effectively present an "infinite" thickness to the beam. In this case, only particles emitted back from the face of the target can be observed. Furthermore, all levels lying above the emitted particle group corresponding to the ground state of that particular reaction for the element making up the backing will be obscured. The target side of the backing should be smooth. Solid backings are usually disks about 1 cm in diameter. The supporting rod is attached at a point along the circumference.

Transparent backings can be penetrated by the incident beam and particles emitted in any direction except along the target face can be observed. The amount of obscuration of energy levels lying near the ground states for that particular reaction in the elements making up the backing will depend on its thickness. In the High Voltage Laboratory, a thin plastic film of Formvar is used as a transparent backing. The backing is produced as follows:

1. Formvar solution is prepared according to the formula:

   1 to 4 grams Formvar E
   100 grams ethylene dichloride
   10 milligrams aerosol
   (Formvar E can be obtained from Shawinigan Resins Corporation, Springfield, Massachusetts.)

2. Using a fine medicine dropper, a drop of Formvar solution is dropped on the surface of distilled water. The drop will spread out because of surface-tension forces, and will dry in an extremely thin film on the surface of the distilled water.

3. This film can be picked up on a standard metal target frame, which is in the form of a hollow rectangle 1 x 2 cm attached to the metal rod described above. The frame is dipped into the water under the surface layer of Formvar and gently raised until the Formvar film forms a sheet across the frame.

If desired, a double layer can be achieved by rotating the target frame 180 degrees during the process of lifting the Formvar film off the water. After the first layer (or double layer) has dried, more layers may be added by repeating the process. A compromise between mechanical durability and thinness is reached by varying the number of layers of Formvar.

The following types of targets have resulted from varying the means employed to lay down a thin layer of the target material on the backing:

1. Painted. The target material is procured in a form that will dissolve in a liquid binder. The requirements of the binder are:

a. It must possess enough body so that it will remain in a smooth film as painted and not be so thin as to tend to form drops that leave the target material clumped in spots when the thinner evaporates; and,

b. It must evaporate with a minimum of contamination.

The organic plastics, Formvar and Zapon, have proved suitable as solvents.

A solid backing of as light an element as possible, for example, graphite or beryllium, is chosen. If the target backing has a rough face, it can be polished with paper until smooth. If pock marks persist, the face receives a coat of pure

Zapon, and the target is baked in a small oven until the Zapon thinner evaporates leaving the pock marks filled in with residue. The same process is then repeated with target material in the Zapon. The solution is painted on the smooth face of the target backing with an ordinary clean camel's hair brush. Thin coats are applied, baking each time between coats. The number of coats will determine the thickness of the target.

2. Sprayed. As in the case of the painted target, the target material is obtained in a soluble form. An artist's spray brush is used to spray a fine mist of the solution onto the surface of either a solid target backing or onto a Formvar target backing. The air pressure and focus used to spray the solution onto a Formvar target backing must be carefully regulated so that the film is not broken and the solution is not wasted.

Clumping of the target material because of droplet formation before evaporation seems to be the chief problem encountered in this method.

3. Deposited Targets. Attempts have been made to deposit a thin layer of the target material on a solid backing by the following method:

a. A flat circular disk of thin beryllium metal was placed on the flat bottom of a small Petri dish especially manufactured for this purpose. The inner diameter of the dish is almost identical to that of the beryllium disk.

b. The target material solution was poured on top of the disk and then allowed to evaporate.

This method failed, because crystallization effects caused the target material to be deposited nonuniformly.

4. Evaporated Targets. Several Formvar target backings are prepared as described above. A bell jar that may be evacuated by associated vacuum equipment encloses a pair of terminal posts 10 inches apart. The target material may be in the form of a wire wound around a tungsten wire between the electrodes, or it may be placed in a conducting boat which is itself connected to the two electrodes. In either case, the target material should be in contact with a high resistance portion of the circuit and should become hot enough to evaporate when current is passed between the electrodes. A metal ring concentric to the target material is supported 2 to 4 inches above the boat by a vertical post. From eight to 10 Formvar backings may be clamped around this ring, inclined toward the center, so as to form an approximately hemispherical ceiling over the material to be evaporated.

After the bell jar is in place and a suitable vacuum achieved, the voltage is gradually raised across the terminals. At a characteristic temperature, the target material will boil off. The target backings receive a coating of target material, the thickness of which can be controlled by varying the time the current is on and the height of the support ring. Glass micro-

scope slides may be placed behind the target frames and their gradually increasing opaqueness serves as an indication of when the targets are of desired thickness.

The evaporation method has proved to be the most successful way of making thin targets. It has the advantage of forming thin uniform targets. Its main disadvantage is that all target materials do not have a low boiling temperature. If extremely high temperatures are required, the heat carried to the Formvar backings by the evaporated material causes them to break before a target layer of the desired thickness can be achieved.

ATTEMPTS TO MAKE RARE-EARTH TARGETS

An original objective was to produce a rare-earth target that would be transparent, thin, uniform, and free from contaminants, and at the same time be capable of withstanding normal length exposures to reasonable beam currents.

The production of a sprayed target of lanthanum was tried. High purity La_2O_3 was dissolved in nitric acid, yielding $La(NO_3)_3 \cdot 6H_2O$ upon the evaporation of the excess HNO_3. The target was heated, changing the compound to the basic nitrate $La(NO_3)_3$. This was purposely done so that further heating of the target by the particle beam in the accelerator would not inadvertently accomplish the same process in the midst of a run. The

basic nitrate was tried as a solution, not only in water, but also in Aquadag (a suspension of graphite in water), and in Formvar in various proportions. These mixtures were then sprayed on Formvar backings. This method failed for a number of reasons. Either the pressure from the spray broke or weakened backings; the drying mixture shrank the Formvar, breaking it; or the surviving targets were too nonuniform. Solid backings (either graphite or beryllium) were also sprayed with various mixtures of target materials and solvents; these likewise proved to be too nonuniform.

The painted targets proved excessively nonuniform and too thick a layer was needed to give the required yield.

Deposited targets were also tried but failed since the layer deposited was nonuniform.

The evaporation technique proved to be the most successful of all the methods employed. At first only the oxides of the rare earths were available in very pure forms. The oxides have very high melting points; therefore, evaporation of these proved to have two main disadvantages. First, target backings were decomposed; second, the metal from the electrodes and other fittings in the vacuum chamber evaporated, contaminating the targets. In order to concentrate the heat in a small volume, a 10 inch x $\frac{1}{2}$ inch spectroscopically pure graphite rod was necked down for about 2 inches in the center of the rod where a hole was drilled for the target material.

This setup failed for three reasons:

1. It did not result in concentrating the heat sufficiently.

2. It fell far short of being rugged enough to withstand either the normal mechanical shocks of careful handling or the stresses set up in uneven heating and cooling.

3. The target material was reduced by the carbon, forming a carbide which refused to evaporate and also electrically shorted the carbon rod.

Some of the rare earths were procured as metals, which, because of their lower boiling points, were much easier to evaporate. A method similar to one described by J. E. Schwager and L. A. Cox[17] was tried. This method consisted in employing two 4 inch x $\frac{1}{2}$ inch carbon rods, one of which had target material embedded in one end, while the other had one end sharpened to a conical tip. These rods were spring-loaded and placed between the electrical terminals with the pointed end of one rod bearing against the material embedded in the other rod. This method failed because the tip became hot and plowed through the soft metal.

The most successful method proved to be a modification of the previously mentioned carbon-boat method. A $\frac{1}{4}$ inch diameter x 2 inch long rod was necked down for a boat and fitted into $\frac{1}{4}$ inch diameter by 3/4 inch deep holes bored into the ends of two 4 inch

by ½ inch diameter carbon rods. This arrangement was clamped between the electrical terminals. This configuration proved to be very rugged and easy to reproduce if broken; it also had the advantage of concentrating the heat the most successfully of any method tried.

Rare-earth targets of varying thickness were produced successfully by this method from the pure metal. The targets proved to be thin, uniform, reasonably free from contaminants, and sufficiently rugged to withstand normal exposure to the beam current. The yield, however, from these targets in a (p,p) reaction proved to be low.

TECHNIQUE OF MAKING THE Mn^{55} TARGET

The evaporation technique was employed successfully in producing a Mn^{55} target. A tantalum boat could be used, since the manganese evaporates at a much lower temperature than does the tantalum. Furthermore, if some tantalum did evaporate and contaminate the target, its much higher Z and A would render it relatively harmless.

To each electrical terminal was attached a 4 inch x ½ inch diameter steel rod. One end of each of the rods was slit, and, by means of set screws, the tantalum boat was firmly connected between the rods. Manganese of 99.99 percent purity was placed in the boat. The following spectroscopic report from Johnson, Matthey and Co., Ltd., the supplier, accompanied the manganese:

"Very faint lines attributed to the following elements were observed: Mg, Cu, Ca. No lines of the following elements were observed: Ag, Al, As, Au, Cd, Co, Cr, Fe, K, Li, Mo, Na, Ni, Pb, Rb, Sb, Sn, Ti, V, W, Zn, and Zr."

Formvar target backings were prepared with three double layers of Formvar on each and were arranged on the supporting ring symmetrically around the boat about 4 inches above it. After the bell jar had been pumped down, voltage was applied gradually across the electrodes until the boat was white hot. The glass slides placed across the target frames were closely observed, and the evaporation process was stopped when light shadows appeared on them. Vacuum was broken gradually in order to prevent breaking the delicate targets, and a few of these first light thin targets were taken out and replaced by fresh Formvar backings, while the remainder were left in place to receive a second coating approximately as heavy as the first. This process was repeated three times, yielding four groups of targets of different thicknesses. This difference was very apparent when the targets were held up to the light.

Using a Fe^{56} target known to be of the proper thickness as a control, it was possible to compare three targets that appeared to bracket it in thickness. The medium target was selected and the $\theta = 60$ degree runs were made on this target. This target

held up under 1000 μc exposure from a rather large beam current, but during a $\theta = 90$ degree run a hole was burned in it. The photographic plates from the 60-degree run were scanned; and, since the target appeared to be slightly thick, the next thinner target was selected for the 30-degree run. This target proved satisfactory in every respect. It was thin, giving narrow, well-resolved peaks. It produced a minimum amount of background and was uniform and relatively free from contaminants. It proved to be rugged in withstanding mechanical shock and exposure to the beam.

APPENDIX II

DETERMINATION OF THE SENSITIVITY OF THE Q EQUATION TO UNCERTAINTIES IN MASS

Suppose a certain proton group, corresponding to an excited level in Mn^{56}, is found for the two different laboratory angles θ_1 = 10 degrees and θ_2 = 30 degrees. Assuming at first no errors in the experiment, we have:

$$Q = \left(\frac{M_T + M_o}{M_T}\right)E_{o_1} - \left(\frac{M_T - M_i}{M_T}\right)E_i - \frac{2\cos\theta_1\sqrt{M_iE_iM_oE_{o_1}}}{M_T} \qquad (1)$$

$$Q = \left(\frac{M_T + M_o}{M_T}\right)E_{o_2} - \left(\frac{M_T - M_i}{M_T}\right)E_i - \frac{2\cos\theta_2\sqrt{M_iE_iM_oE_{o_2}}}{M_T} \qquad (2)$$

where M_T is the mass of Mn^{56}, all symbols have the same meanings as in Part III, and M_T, M_o, M_i, E_i, and Q remain constant. Equating Eqs. (1) and (2), we have:

$$(E_{o_1} - E_{o_2})\left(\frac{M_T + M_o}{M_T}\right) = \frac{2(M_iE_iM_o)^{\frac{1}{2}}}{M_T}\left(\sqrt{E_{o_1}}\cos\theta_1 - \sqrt{E_{o_2}}\cos\theta_2\right)$$

$$\sqrt{E_{o_1}}\cos\theta_1 - \sqrt{E_{o_2}}\cos\theta_2 = \frac{M_T + M_o}{2(M_iE_iM_o)^{\frac{1}{2}}}(E_{o_1} - E_{o_2}) \qquad (3)$$

Next, let us attempt to assign the same values E_{o_1} and E_{o_2} to some nuclide other than Mn^{56} where M_T' denotes its mass.

We now write:

$$Q_1 = \left(\frac{M_r' + M_o}{M_r'}\right)E_{o_1} - \left(\frac{M_r' - M_i}{M_r'}\right)E_i - \frac{2\cos\theta_1\sqrt{M_iE_iM_oE_{o_1}}}{M_r'} \qquad (4)$$

$$Q_2 = \left(\frac{M_r' + M_o}{M_r'}\right)E_{o_2} - \left(\frac{M_r' - M_i}{M_r'}\right)E_i - \frac{2\cos\theta_2\sqrt{M_iE_iM_oE_{o_2}}}{M_r'} \qquad (5)$$

where $Q_1 \neq Q_2$ since the nuclide in question is not Mn^{56}.

Solving (4) and (5) simultaneously, we have:

$$\Delta Q = Q_1 - Q_2 = \left(\frac{M_r' + M_o}{M_r'}\right)(E_{o_1} - E_{o_2})$$

$$- \frac{2\sqrt{M_iE_iM_o}}{M_r'}(\cos\theta_1\sqrt{E_{o_1}} - \cos\theta_2\sqrt{E_{o_2}}) \qquad (6)$$

Substituting (3) in (6):

$$\Delta Q = \left(\frac{M_r' + M_o}{M_r'}\right)(E_{o_1} - E_{o_2})$$

$$- \frac{2\sqrt{M_iE_iM_o}}{M_r'}\left[\frac{M_r + M_o}{2\sqrt{M_iE_iM_o}}(E_{o_1} - E_{o_2})\right]$$

$$\Delta Q = \left(\frac{M_r' + M_o}{M_r'}\right)(E_{o_1} - E_{o_2}) - \left(\frac{M_r + M_o}{M_r'}\right)(E_{o_1} - E_{o_2})$$

$$\Delta Q = \left(\frac{M_r' - M_r}{M_r'}\right)(E_{o_1} - E_{o_2}) \qquad (7)$$

Solving for M_r':

$$M_r' = \frac{(E_{o_1} - E_{o_2})M_r}{(E_{o_1} - E_{o_2}) \pm \Delta Q} .$$

Now, if we say that our error in Q is 10 kev, we can find the uncertainty in mass resulting from this error for any distance, d, along the plate, say: $d_1 = 79$ for $\theta_1 = 10$ degrees. Entering the Q-value tables computed by the IBM 650 and interpolating, we have:

θ = 10 degrees	θ = 30 degrees
d = 79.00 cm	d = 79.25 cm
Q = 5216 kev	Q = 5216 kev
E_{o_1} = 12,217 kev	E_{o_2} = 12,161 kev

$$M_r' = \frac{(E_{o_1} - E_{o_2})\, M_r}{(E_{o_1} - E_{o_2}) \pm \Delta Q} = \left(\frac{56}{56 \pm 10}\right)M_r$$

$$M_r' = \frac{56}{66}\ (56) \quad \text{or} \quad \frac{56}{46}\ (56)$$

$$M_r' = 47.5 \quad \text{or} \quad 68.2$$

BIBLIOGRAPHY

1. A. B. Martin, Phys. Rev. 71, 127 (1947); 72, 378 (1947).
2. A. Y. Abramov, Doklady Akad. Nauk. USSR, 73 (No. 5), 921 (1950); and Nuclear Science Abstracts, Vol. 4, No. 22, A6435 (1950).
3. W. D. Whitehead and N. P. Heydenburg, Phys. Rev. 79, 99 (1950).
4. B. Hamermesh and V. Hummel, Phys. Rev. 83, 663 (1951); 88, 916 (1952).
5. G. A. Bartholomew and B. B. Kinsey, Phys. Rev. 89, 390 (1953).
6. M. Reier and M. H. Shamos, Phys. Rev. 95, 636 (1954).
7. K. Way, L. W. King, C. L. McGinnis, E. van Lushout, Nuclear Level Schemes (TID-5300), USAEC, GPO (1955).
8. W. W. Buechner, A. Sperduto, C. P. Browne, and C. K. Bockelman, Phys. Rev. 91, 1502 (1953).
9. W. W. Buechner, M. Mazari, and A. Sperduto, Phys. Rev. 101, 188 (1956).
10. H. A. Enge, Rev. Sci. Inst. 23, 599 (1952).
11. K. T. Bainbridge, Experimental Nuclear Physics (Segre), Vol. I, John Wiley and Sons, Inc., New York, 1953. p. 669.
12. K. T. Bainbridge, Experimental Nuclear Physics (Segre), Part V. ibid. p. 745.
13. S. F. Zimmerman, Jr. "Focusing Properties of a High-resolution, Magnetic Spectrograph," M.I.T. Master's Thesis (1955).
14. H. A. Enge, "Table of Charged-particle Energies versus Magnetic Field Strength X Orbit Radius," A. S. John Griegs, Bergen, Norway (1954).
15. H. A. Enge, private communication.

16. H. A. Enge, "On Heavy Particle Spectroscopy Technique, Its Application to Scattering Mass Analysis and to the $Al^{27}(d,\alpha)Mg^{25}$ and $Al^{27}(d,p)Al^{28}$ Reactions," University of Bergen (Norway)(1954), pp. 74-77.

17. J. E. Schwager and L. A. Cox, Rev. Sci. Inst. 24, 986 (1953).